

## Zeeman Effect of the Forbidden Lines of Pb I

### I. Pure Quadrupole and Magnetic Dipole Lines

F. A. JENKINS AND S. MROZOWSKI

*Department of Physics, University of California, Berkeley, California*

(Received March 17, 1941)

A very intense source of the forbidden lines, consisting of a high frequency discharge through helium containing a small amount of lead vapor, is used to photograph the Zeeman patterns in fields up to 4000 gauss. Reproductions are given of the transverse effect for the main hyperfine component, due to the even isotopes, in a magnetic dipole line,  $\lambda 4618$ , and in two quadrupole lines,  $\lambda 4659$  and  $5313$ . The reversal of polarization in  $\lambda 4618$  is clearly shown. The splittings of the weaker hyperfine components emitted by  $\text{Pb}^{207}$  are also observed for  $\lambda 5313$  and  $4618$ , including, in the latter case, fields strong enough to show the Back-Goudsmit effect. Splittings and intensities are in satisfactory agreement with theory throughout. These are the first observations on the Zeeman effect of the hyperfine structure of forbidden lines, and they establish the applicability of the electric dipole intensity formulas (with interchange of polarization) to magnetic dipole lines and of the Rubinowicz quadrupole formulas (with suitable substitutions of quantum numbers) to quadrupole lines.

IN a previous paper,<sup>1</sup> one of us has described a very intense source of the forbidden lines of lead that are emitted in transitions between the levels of the normal ( $6p^2$ ) configuration. It was possible to investigate the hyperfine structure due to  $\text{Pb}^{207}$  in the case of three of these lines, and to measure the relative intensities of the five lines observed. According to the selection rules, the strongest line,  $\lambda 4618$  ( $^1S_0 \rightarrow ^3P_1$ ) is permitted only for magnetic dipole radiation, two others,  $\lambda 5313$  ( $^1S_0 \rightarrow ^3P_2$ ) and  $\lambda 4659$  ( $^1D_2 \rightarrow ^3P_0$ ) only for electric quadrupole, while the remaining ones,  $\lambda 7330$  ( $^1D_2 \rightarrow ^3P_1$ ) and  $\lambda 9250$  ( $^1D_2 \rightarrow ^3P_2$ ) involve both types of radiation. Since the existing data on the Zeeman effect of forbidden lines are rather meager, and in no case include the hyperfine structure, it seemed worth while to investigate the effect in these lines.

The Zeeman effect of  $\lambda 4618$  has been studied by Niewodniczanski<sup>2</sup> and this constitutes the only existing example of the effect in a pure magnetic dipole line. With our improved source we obtained the line with an intensity at least 500 times greater than that attained by Niewodniczanski. This made it possible to observe the Zeeman effect not only for the strong central component due to the even isotopes of masses

204, 206 and 208, but also for the much weaker hyperfine components due to the odd isotope, 207. The same was true for the pure quadrupole line  $\lambda 5313$ , even though this is some five times weaker than  $\lambda 4618$ . For the other, still weaker quadrupole line,  $\lambda 4659$ , only the central component could be studied. Of the two mixed lines, the stronger one at  $\lambda 7330$  has been investigated in detail, including quantitative intensity measurements of the Zeeman components. In Part I of this paper we shall give the results on the pure quadrupole and magnetic dipole lines, while the case of the mixed line, in which a new interference effect between the two types of radiation has been discovered, will be considered later in Part II.

#### EXPERIMENTAL

The lines were excited by a high frequency discharge in helium containing a small amount of lead vapor. The characteristics of this source have already been described in some detail,<sup>1</sup> so it will only be necessary to give here the modifications which became necessary for its operation in a magnetic field. Figure 1 shows, to scale, the cylindrical quartz discharge tube  $T$  and the asbestos-insulated Nichrome oven  $F$  situated between the poles  $P, P$  of the magnet. For large fields it is necessary to have the discharge current in the direction of the field, so in

<sup>1</sup> S. Mrozowski, Phys. Rev. **50**, 1086 (1940).

<sup>2</sup> H. Niewodniczanski, Acta Phys. Polonica **3**, 285 (1934).

this case the high frequency potential was applied to external electrodes  $E, E$  consisting of strips of platinum 5 mm wide placed above and below the tube. This disposition of the electrodes has the advantage that the deposit of carbon which gradually forms near the electrodes<sup>1</sup> does not occur on the window. The intensity with which the forbidden lines can be produced is, however, much less than with the previous arrangement using ring-shaped electrodes near the ends of the tube. The loss of intensity is due to the fact that when one approaches the best conditions for the forbidden lines (high helium pressure, or high vapor pressure of lead), the bright part of the discharge splits in a strong magnetic field into two regions close to the electrodes, leaving the middle with fairly low luminosity. This is no doubt caused by the spiraling of the electrons around the magnetic lines of force, which leads to an increase of ionization near the electrodes, and a more intense emission of the allowed lines in these regions. The forbidden lines, however, are emitted with nearly uniform intensity across the space between the electrodes, as a result of the diffusion of metastable atoms. These lines could be easily distinguished visually from the allowed lines by this difference in intensity distribution. The best conditions for the lines investigated here were a helium pressure of 4 to 5 mm and a temperature somewhat below 800°C, such that the Pb II lines are still very bright and the He lines have not yet disappeared completely.

With the smaller magnetic fields used in investigating the Zeeman effect of the hyperfine structure, the ring-type electrodes could be used, and gave an intensity of the forbidden lines even greater than that obtained without magnetic field. At a field greater than about 1000 gauss, the discharge concentrates at each end toward certain points inside the electrodes. The resulting increase in current density destroys the metastable atoms, and although the intensity of all allowed lines increases with further increase of the magnetic field, the forbidden lines become weaker.

The magnet used<sup>3</sup> could give a field of 4000

<sup>3</sup>A. V. Hershey, Phys. Rev. **56**, 908 (1939). Thesis, University of California, 1939.

gauss constant to within one percent over the space occupied by the tube. Since the oven had to be maintained at a high temperature over long periods of time,<sup>1</sup> water-cooled copper plates were placed over the pole faces to prevent overheating of the magnet when it was not in operation. The optical apparatus, consisting of a one-prism glass spectrograph and silvered quartz Fabry-Perot plates, were the same as those used in the previous work.

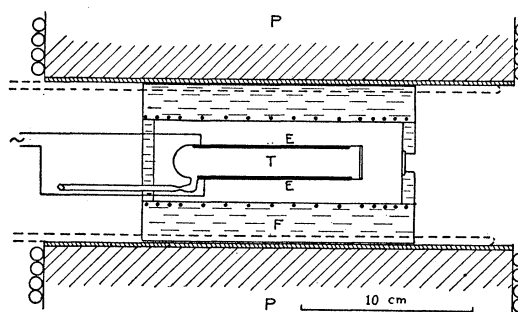


FIG. 1. Arrangement of the source.

Measurements of the Zeeman splittings were made on a comparator, including several orders of each Fabry-Perot pattern. By interpolation on a parabolic curve, linear distances were expressed as fractions of the separation of orders, and for each component the average fraction from the different orders was then converted to wave numbers.

For the calibration of the magnetic field, the Zeeman splitting of the singlet line  $\lambda 4916$  ( $6^1P_1 - 8^1S_0$ ) of mercury was carefully measured at six different values of the field. The mercury spectrum was excited with the same apparatus by merely introducing mercury vapor into the tube. With  $\Delta\nu = 4.67 \times 10^{-5}$  Hg, and with  $g = 1.010$  for this line,<sup>4</sup> values of  $H$  were found which were accurately proportional to the current in the magnet.

## RESULTS

### Zeeman effect of the main components

From both the experimental and theoretical sides, the investigation of the Zeeman effect of the main component due to the even isotopes is much simpler. As was shown by Mrozowski,<sup>1</sup>

<sup>4</sup>P. Gmelin, Ann. d. Physik **28**, 1079 (1909).

this component contains 79 percent of the intensity of each line, in agreement with the abundance of the isotopes. Its Zeeman pattern could be photographed with relatively short exposures (30 sec. in the case of  $\lambda 4618$ ) while the pattern for the hyperfine components emitted by the odd isotope required more than ten times this exposure, and was partly overlapped by the main pattern. Because of this overlapping, no quantitative intensity measurements were attempted for the patterns reported here, but a qualitative comparison with theory gives an important conclusion mentioned below.

The fourth column of Table I gives the results of measurements on the main patterns. The magnetic dipole line  $\lambda 4618$  gives a  $\frac{3}{2}$ -normal triplet, but with the center component polarized perpendicular to the field, the outer ones parallel. This reversal of the normal polarization is shown very clearly in Fig. 2(b), where the line can at once be distinguished from electric dipole lines by this characteristic. This photograph was obtained by consecutive illumination of the two halves of the slit of the spectrograph with light of different polarization. The exposure time in the  $\pi$  case was made twice as long as in the other in order to equalize the blackenings in the line  $\lambda 4618$ . This explains why the  $\pi$  components of the neighboring electric dipole lines appear so strong in comparison to the  $\sigma$  components. The  $\sigma$  component of  $\lambda 4618$  nearly overlaps with a  $\pi$  component of a neighboring electric dipole line. The reversal of the normal polarization has already been observed by Niewodniczanski,<sup>2</sup> but the reproduction of the line in his article was not satisfactory. According to the theory<sup>5</sup> the magnetic dipole radiation field is obtained from the electric dipole case by substituting  $\mathbf{H}$  for  $\mathbf{E}$  and  $-\mathbf{E}$  for  $\mathbf{H}$  and by replacing the electric moment by the magnetic moment. Hence the selection and intensity rules for the Zeeman effect of

magnetic dipole lines are the same as for electric dipole lines, but with the polarizations interchanged. Thus our result gives convincing evidence for the magnetic dipole character of this line.

The two quadrupole lines give a characteristic pattern of four lines of equal intensity (Fig. 2(d) and (f)), corresponding to  $\Delta M = \pm 1(\pi)$  and  $\pm 2(\sigma)$ . The transition  $\Delta M = 0$  is also allowed, but has zero intensity for either transverse or longitudinal observation, appearing only as an elliptically polarized component in diagonal observation.<sup>6</sup> The calculated splittings given in the last column of Table I were obtained by using the  $g$  values determined by Back<sup>7</sup> from the allowed lines involving these levels, namely for  $^3P_0$  and  $^1S_0$ , 0/0, for  $^3P_1$ , 1.501, for  $^3P_2$ , 1.269, and for  $^1D_2$ , 1.230. It will be seen that our observed splittings are consistently a little lower than the computed ones. This may possibly be due to the fact that the  $g$  value we adopted for the calibrating Hg line  $\lambda 4916$  was a little too small.<sup>8</sup> Our measurements were quite accurate for the lines  $\lambda 4618$  and  $\lambda 5313$ , but somewhat less reliable for  $\lambda 4659$ , because here the components were not as sharp and were partly overlapped by neighboring lines.

### Zeeman effect of the hyperfine structure

We have been able for the first time to observe the effect of a magnetic field on the hyperfine structure of forbidden lines. The two cases  $\lambda 4618$  (magnetic dipole) and  $\lambda 5313$  (quadrupole) were investigated. Reproductions of the spectrograms appear in Fig. 2(c) and (e), and the results of the measurements are presented graphically in Fig. 3. For  $\lambda 4618$ , because of its greater intensity and smaller hyperfine splitting, observations could be carried to large enough fields to show the Back-Goudsmit ("strong field") effect, while for  $\lambda 5313$  only the "weak field" effect could be studied.

In obtaining the theoretical patterns in Fig. 3, the splitting factors of the levels for weak fields

TABLE I. Zeeman patterns of the main components.

$\lambda$	TRANSITION	RADIATION	OBS.	CALC.
4659.18	$^1S_0 \rightarrow ^3P_1$	Magnetic dipole	0 (1.48)	0 (1.501)
5313.00	$^1S_0 \rightarrow ^3P_0$	Quadrupole	(1.23) 2.53	(1.269) 2.538
4659.02	$^1D_2 \rightarrow ^3P_0$	Quadrupole	(1.20) 2.45	(1.23) 2.46

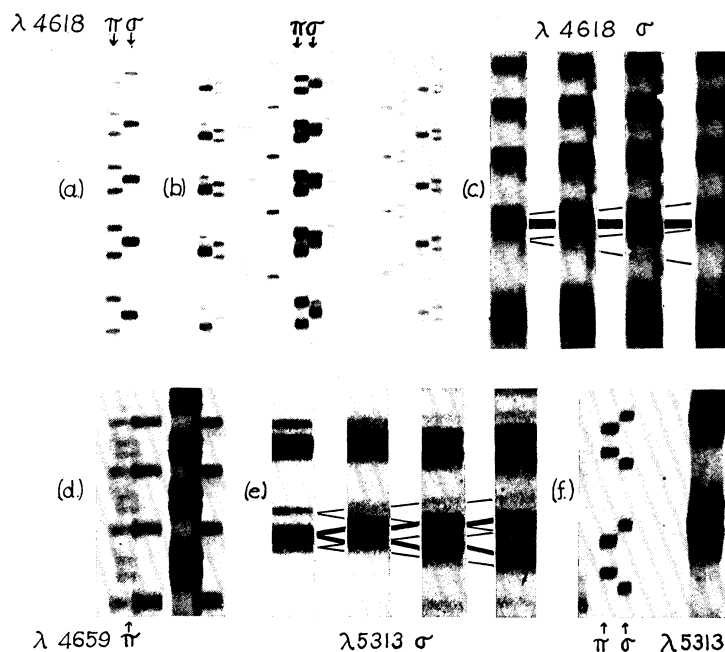
<sup>5</sup> A. Sommerfeld, *Atombau und Spektrallinien* (1939), Vol. 2, p. 735.

<sup>6</sup> E. Segrè and C. J. Bakker, *Zeits. f. Physik* **72**, 724 (1931).

<sup>7</sup> E. Back, *Zeits. f. Physik* **37**, 193 (1926).

<sup>8</sup> On the Hg spectrograms the singlet line  $\lambda 5790$  ( $6^1P_1 - 7^1D_2$ ) was also measured, and showed a splitting 8 percent greater than  $\lambda 4916$ . This does not agree with Gmelin,<sup>4</sup> who concluded that  $\lambda 5790$  gave a normal triplet.

FIG. 2. Zeeman patterns of the forbidden lines. (a)  $\lambda 4618$ .  $H=2875$  gauss; 5-mm spacer; exposures 50 sec. (b)  $\lambda 4618$  and adjacent electric dipole lines.  $H=2890$  gauss; 3.5-mm spacer; exposures 40 min. and 20 min. (c)  $\lambda 4618$ ,  $\sigma$  components only, showing hyperfine structure.  $H=0, 670, 1090$  and  $1590$  gauss; 15-mm spacer; exposure 4 min. for  $H=0$ , 15 min. for the others. (d)  $\lambda 4659$ ,  $\pi$  components. The arrow indicates the pattern for this weak line, which is overlapped by strong adjacent lines. Exposure 45 min. (e)  $\lambda 5313$ ,  $\sigma$  components showing hyperfine structure  $H=0, 225, 500, 765$  gauss; 9-mm spacer; exposures 1 hour, 30 min. (f)  $\lambda 5313$ ,  $\pi$  and  $\sigma$  components.  $H=2890$  gauss; 3.5-mm spacer; exposures 40 min.



were obtained from the Goudsmit formula

$$G_F = G_J \frac{F(F+1) - J(J+1) - I(I+1)}{2F(F+1)}$$

For strong fields, the splitting due to the nuclear moment is given by  $AM_I M_J$ , the coupling constant  $A$  being determined from the hyperfine splittings of the levels without field, namely  $\Gamma_F = \frac{1}{2}A[F(F+1) - J(J+1) - I(I+1)]$ . (The over-all separation of the hyperfine structure,  $\Delta\nu = \frac{1}{2}A[F_{\max}(F_{\max}+1) - F_{\min}(F_{\min}+1)] = AI(2J+1)$ , if  $J > I$ .) The splitting in intermediate fields could have been calculated exactly from the theoretical equations. However, since only the weak field effect was observed for  $\lambda 5313$ , and since for  $\lambda 4618$  the hyperfine splitting is small and not known very precisely, this calculation was not made. Instead, a graphical interpolation between the weak and strong field levels was used, since this should give the transition effect within the accuracy justified by our measurements.

The upper diagram of Fig. 3 shows the predicted and observed splittings for the magnetic dipole line,  $\lambda 4618$ , including both polarizations. The upper level,  $^1S_0$ , does not split, so that the diagram gives directly the splitting of the lower

state,  $^3P_1$ . In the theoretical weak field patterns of the hyperfine structure components, for which the separations and intensities are indicated at the left of the figure, it will be seen that all components except the outer  $\pi$  components in the high frequency member of the hyperfine doublet should appear in both polarizations. The agreement between experiment and theory is complete, both as to separations and intensities. Since the theoretical intensities are those calculated from the ordinary electric dipole formulas, we see that one can extend to the hyperfine structure the rule that everything is the same as in the electric dipole case, but with reversed polarizations. At the highest fields reached, the Back-Goudsmit effect is almost complete, and here also the observations agree satisfactorily, though they are rather incomplete.

The lower diagrams of Fig. 3 show the results for the quadrupole line  $\lambda 5313$ . In this case also ( $^1S_0 \rightarrow ^3P_2$ ), the splittings are those of the lower state. Because the pattern is more complicated, the  $\pi$  and  $\sigma$  components are plotted separately in parts (a) and (b) of the figure. The theoretical intensities for weak fields were obtained from the Rubinowicz formulas<sup>9</sup> by substituting  $F$  for  $J$ .

<sup>9</sup> A. Rubinowicz and J. Blaton, *Ergeb. d. exakt. Naturwiss.* **11**, 176 (1932).

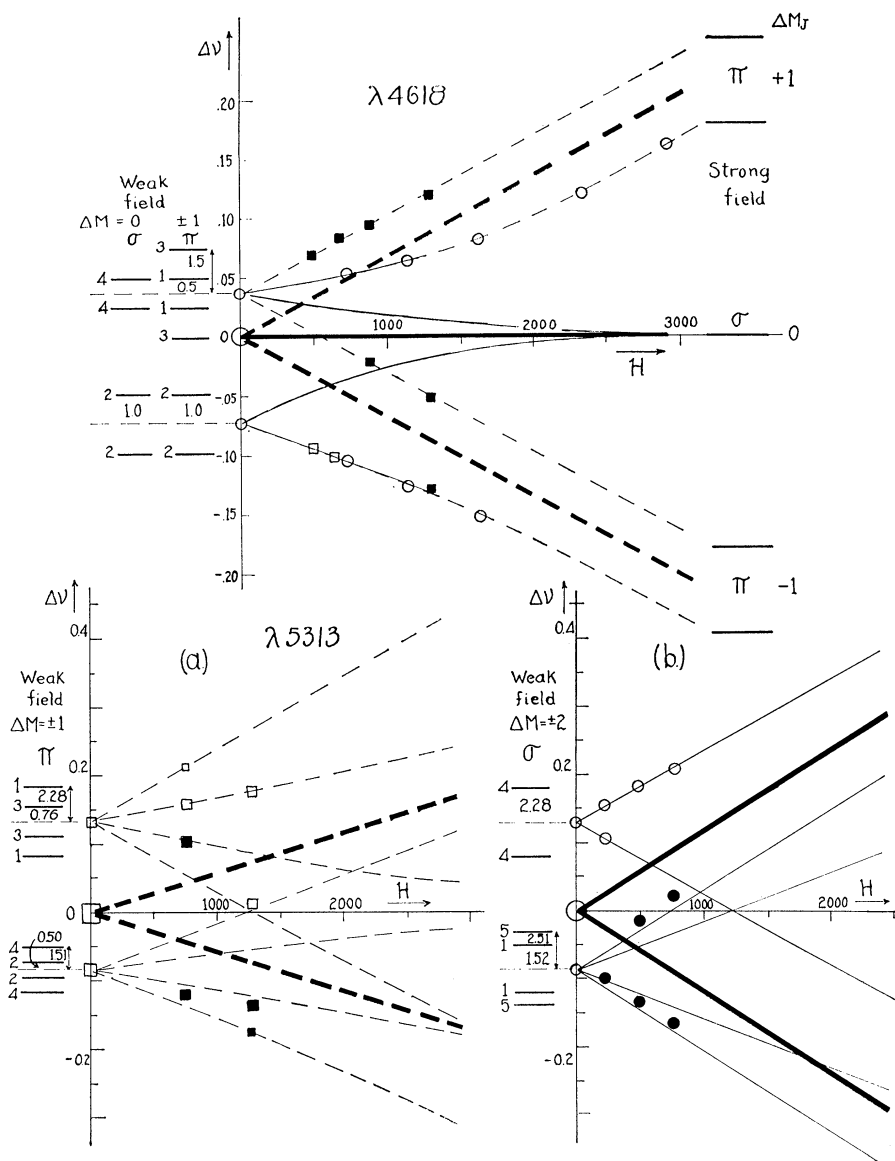


FIG. 3. Predicted and observed splittings for the magnetic dipole line  $\lambda 4618$  (upper diagram) and for the quadrupole line  $\lambda 5313$  (lower diagram). In both cases since the upper level  $^1S_0$  does not split, the diagrams give directly the splitting of the lower states. The heavy lines refer to the main component; the lighter ones to the hyperfine structure. Broken lines are the parallel components; the solid lines the perpendicular ones. Squares represent components observed in  $\pi$  polarization; circles those in  $\sigma$ . Open squares or circles are for lines observed as completely resolved from the main pattern while filled ones are for those which are in contact with or partly overlapped by the main components.

Since the hyperfine structure is considerably wider in this case, we could not reach fields large enough to show the Back-Goudsmit effect. This line is much weaker and in order to get the hyperfine structure components on not too long exposed plates the ring-type electrodes had to be used. Within the range of magnetic fields used, the observed pattern agrees well with that predicted for weak fields. The applicability of the modified Rubinowicz formulas to the Zeeman effect in the hyperfine structure of a quadrupole line is thus verified for the first time. Not only do

we observe the lines  $\Delta M = \pm 2$  in the perpendicular effect, and  $\Delta M = \pm 1$  in parallel, but also the intensities are qualitatively right for the quadrupole case. For example, the highest frequency  $\pi$  component is considerably weaker than the next one (as indicated by the smaller open square in Fig. 3(a)), corresponding to the predicted ratio 1 to 3. The intensity formulas for electric dipole give just the reverse ratio, 3 to 1, for these two lines.

The only feature of our pattern which does not agree with the theory for weak fields is the in-

tensity of the lowest frequency  $\pi$  component (smaller filled square in Fig. 3(a)), which is apparently much weaker than it should be. This may possibly be explained as an incipient Back-Goudsmit effect, since the line goes to zero intensity in strong fields and the effect is observed at the highest field we used for this line.

The apparent weakness of this component is probably enhanced by the fact that the next component lies on the wing of a main line, and therefore looks relatively too strong. In any case, there is no reason here to doubt the validity of the existing theory of the Zeeman effect of quadrupole lines.

MAY 15, 1941

PHYSICAL REVIEW

VOLUME 59

## The Dynamics of a Particle in General Relativity

C. LANZOS

*Purdue University, Lafayette, Indiana*

(Received September 12, 1940)

Some applications of the Gaussian integral transformation to the conservation law of the matter tensor yield the complete dynamical law for a material particle in a Riemannian space, in the form of two relations which correspond completely to Newton's two fundamental laws. The "moving force" of the motion law comes out as a volume integral which can be transformed into a surface integral. The inertial mass and the coordinates of the center of mass, on the other hand, are genuine volume integrals which cannot be transformed into boundary integrals. For weak and static matter the principle of the geodesic line can be established, irrespective of spherical symmetry. But even for static and infinitesimal matter an interesting exception occurs if the total mass of the particle happens to drop

down to a quantity of second order, as is indeed the case if the scalar condition  $T=0$  is satisfied inside of the particle. Then the acceleration is smaller than it should be according to the geodesic principle which has the consequence that the gravitational mass of the sun, determined in the customary manner by the acceleration of its planets, may be underestimated. This gives a new clue for the understanding of the anomalous value of the light deflection on the limb of the sun, discovered by Freundlich and his collaborators. However, the theoretical prediction of an increase of 83 percent, deduced for a static and spherically symmetric particle, is too large in comparison with the 25-40 percent increase, indicated by Freundlich's measurements.

### I. INTRODUCTION

EVER since the discovery of general relativity the question of the motion of a particle in a Riemannian field has been raised and discussed. The original paper of Einstein<sup>1</sup> went a long way toward the establishment of a field dynamics, by showing that the matter tensor of general relativity satisfies the conservation laws of energy and momentum as a mathematical necessity. He also succeeded in bringing that conservation law rigorously into the form of a classical divergence equation, by adding to the matter tensor certain auxiliary quantities which had no invariant significance but were interpretable as the momentum-stress-tensor of the gravitational field.<sup>2</sup>

However, the conservation law of momentum

and energy in itself is not able to establish a motion law for the material particle. The mechanics of discrete points is based on the two fundamental announcements of Newton: (a) momentum equals mass times velocity; (b) the time rate of change of momentum equals moving force. If we have to reinterpret these laws in terms of field quantities, the *second* law offers no difficulties. The conservation law of momentum can be considered as the direct counterpart of the second law of Newton. The real difficulty lies in the *first* law, *viz.* in finding a kinematic interpretation for the momentum of the field.

In an earlier attempt<sup>3</sup> the author was able to solve the motion problem of a particle for the case of special relativity. The method is based on the application of the Gaussian integral

<sup>1</sup> A. Einstein, Ann. d. Physik 49, 769 (1916).

<sup>2</sup> Cf. reference 1, p. 809.

<sup>3</sup> C. Lanczos, Zeits. f. Physik 59, 514 (1930).

FIG. 2. Zeeman patterns of the forbidden lines. (a)  $\lambda 4618$ .  $H=2875$  gauss; 5-mm spacer; exposures 50 sec. (b)  $\lambda 4618$  and adjacent electric dipole lines.  $H=2890$  gauss; 3.5-mm spacer; exposures 40 min. and 20 min. (c)  $\lambda 4618$ ,  $\sigma$  components only, showing hyperfine structure.  $H=0, 670, 1090$  and  $1590$  gauss; 15-mm spacer; exposure 4 min. for  $H=0$ , 15 min. for the others. (d)  $\lambda 4659$ ,  $\pi$  components. The arrow indicates the pattern for this weak line, which is overlapped by strong adjacent lines. Exposure 45 min. (e)  $\lambda 5313$ ,  $\sigma$  components showing hyperfine structure  $H=0, 225, 500, 765$  gauss; 9-mm spacer; exposures 1 hour, 30 min. (f)  $\lambda 5313$ ,  $\pi$  and  $\sigma$  components.  $H=2890$  gauss; 3.5-mm spacer; exposures 40 min.

